Inorg. Chem. **2003**, *42*, 5989–5998

A Phosphorus Supported Multisite Coordinating Tris Hydrazone $P(S)[N(Me)N{=}CH{-}C_6H_4\text{-}o\text{-}OH]_3$ as an Efficient Ligand for the Assembly of Trinuclear Metal Complexes: Synthesis, Structure, and Magnetism

Vadapalli Chandrasekhar,*,† Ramachandran Azhakar,† Gurusamy Thanagavelu Senthil Andavan,† Venkatasubbaiah Krishnan,† Stefano Zacchini,‡ Jamie F. Bickley,‡ Alexander Steiner,‡ Raymond J. Butcher,§ and Paul Kögerler||

Department of Chemistry, Indian Institute of Technology, Kanpur-208 016, India, Department of Chemistry, University of Liverpool, Liverpool-L69 7ZD, U.K., Department of Chemistry, Howard University, Washington, D.C. 20059, and Ames Laboratory and Department of Physics & Astronomy, Iowa State University, Ames, Iowa 50011

Received April 23, 2003

A phosphorus supported multisite coordinating ligand $P(S)[N(Me)N{=}CH{-}C_6H_4\text{-}o\text{-}OH]_3$ (**2**) was prepared by the condensation of the phosphorus tris hydrazide $P(S)[N(Me)NH_2]_3$ (**1**) with *o*-hydroxybenzaldehyde. The reaction of **2** with $M(OAc)_2{\cdot}xH_2O$ (M = Mn, Co, Ni, $x = 4$; M = Zn, $x = 2$) afforded neutral trinuclear complexes $\{P(S)[N(Me)N{=}CH{-}C_6H_4\text{-}o\text{-}O]_3\}_2M_3$ [M = Mn (**3**), Co (**4**), Ni (**5**), and Zn (**6**)]. The X-ray crystal structures of compounds **2**–**6** have been determined. The structures of **3**–**6** reveal that the trinuclear metal assemblies are nearly linear. The two terminal metal ions in a given assembly have an N_3O_3 ligand environment in a distorted octahedral geometry while the central metal ion has an O_6 ligand environment also in a slightly distorted octahedral geometry. In all the complexes, ligand **2** coordinates to the metal ions through three imino nitrogens and three phenolate oxygens; the latter act as bridging ligands to connect the terminal and central metal ions. The compounds **2**–**6** also show intermolecular C—H···S=P contacts in the solid-state which lead to the formation of polymeric supramolecular architectures. The observed magnetic data for the $(s = {}^5/_2)_3$ $L_2(Mn(II))_3$ derivative, **3**, show an antiferromagnetic nearest- and next-nearest-neighbor exchange ($J = -4.0$ K and $J' = -0.15$ K; using the spin Hamiltonian $\hat{H}_{HDvV} = -2J(\hat{S}_1\hat{S}_2 + \hat{S}_2\hat{S}_3) - 2J'\hat{S}_1\hat{S}_3$). In contrast, the $(s = 1)_3$ $L_2(Ni(II))_3$ derivative, **5**, displays ferromagnetic nearest-neighbor and antiferromagnetic next-nearest-neighbor exchange interactions ($J = 4.43$ K and $J' = -0.28$ K; $\hat{H} = \hat{H}_{HDvV} + \hat{S}_1D\hat{S}_1 + \hat{S}_2D\hat{S}_2 + \hat{S}_3D\hat{S}_3$). The magnetic behavior of the $L_2(Co(II))_3$ derivative, **4**, reveals only antiferromagnetic exchange analogous to **3** ($J = -4.5$, $J' = -1.4$; same Hamiltonian as for **3**).

Introduction

The assembly of tailor-made ligand systems that can generate metal complexes of specific nuclearity, coordination number, and geometry is an endeavor of considerable and continued interest to inorganic and organometallic chemists.[1–3] The pyrazolyl borate family of ligands also known as scorpionates has been remarkably successful because of several reasons:[4] (a) they are readily synthesized in excellent yields in a one-step synthesis, (b) they form robust complexes with a variety of transition metal and lanthanide metal ions, and (c) their steric and electronic properties can be readily modulated to suit specific needs of the metal ions that they bind. Recently, other types of trianionic ligands are also being explored.[5] We have been interested in developing multisite ligand systems that are supported on phosphorus.[6] Our

* To whom correspondence should be addressed. E-mail: vc@iitk.ac.in. Phone: 91-512-2597259. Fax: 91-512-2590007/2597436.
† Indian Institute of Technology.
‡ University of Liverpool.
§ Howard University.
|| Iowa State University.

(1) (a) Kottke, T.; Stalke, D. *Chem. Ber./Recl.* **1997**, *130*, 1365. (b) Fleischer, R.; Stalke, D. *Coord. Chem. Rev.* **1998**, *176*, 431. (c) Mahalakshmi, L.; Stalke, D. *Struct. Bonding* **2002**, *103*, 85. (d) Wingerter, S.; Pfeiffer, M.; Murso, A.; Lustig, C.; Stey, T.; Chandrasekhar, V.; Stalke, D. *J. Am. Chem. Soc.* **2001**, *123*, 1381.
(2) Chandrasekhar, V.; Nagendran, S. *Chem. Soc. Rev.* **2001**, *30*, 193.
(3) Steiner, A.; Zacchini, S.; Richards, P. I. *Coord. Chem. Rev.* **1998**, *176*, 431.

10.1021/ic034434h CCC: $25.00
Published on Web 08/20/2003

experience on phosphorus pyrazolides $P(O)(3,5\text{-}Me_2Pz)_3$,[6a] $MeP(S)(3,5\text{-}Me_2Pz)_2$,[6b] or $PhP(O)(3,5\text{-}Me_2Pz)_2$[6c] has shown that these ligands undergo facile P−N bond hydrolysis after the interaction of the ligand with the transition metal ion. In order to assemble robust multisite ligands, we looked at phosphorus hydrazides as attractive alternatives. Acyclic phosphorus hydrazides of the type $PhP(O)[N(Me)NH_2]_2$ have been used extensively by Majoral and co-workers for preparing a large variety of macrocycles.[7] Katti and co-workers have extensively studied these acyclic phosphorus hydrazides for interaction with transition metal ions and have elegantly delineated their interesting coordination chemistry.[8] These simple acyclic phosphorus hydrazides with their reactive terminal NH_2 groups are amenable for ready modification and serve as ideal platforms for elaboration into complex multisite coordination ligands. We have chosen the trihydrazide $P(S)[N(Me)NH_2]_3$ (**1**) with its three NH_2 end groups as our starting precursor and have converted it into the tris hydrazone $P(S)[N(Me)N{=}CH{-}C_6H_4\text{-}2\text{-}OH]_3$ (**2**), LH_3. The tris hydrazone LH_3 has been found to be an excellent ligand for specific assembly of trinuclear metal complexes. In the following account, we describe the synthesis and structure of LH_3 (**2**) and the trinuclear metal derivatives L_2M_3 [M = Mn(II) (**3**), Co(II) (**4**), Ni(II) (**5**), and Zn(II)(**6**)]. The magnetic studies on these trinuclear derivatives are also described.

Experimental Section

Reagents and General Procedures. Solvents and other general reagents used in this work were purified according to standard procedures.[9] $P(S)Cl_3$ and salicylaldehyde (Fluka, Switzerland) were used as purchased. *N*-Methylhydrazine was obtained as a gift from the Vikram Sarabhai Space Research Centre, Thiruvananthapuram, India, and used as such. $Mn(OAc)_2{\cdot}4H_2O$, $Co(OAc)_2{\cdot}4H_2O$, $Ni(OAc)_2{\cdot}4H_2O$, and $Zn(OAc)_2{\cdot}2H_2O$ were obtained from S.D. Fine Chemicals, Mumbai, India.

Instrumentation. Electronic spectra were recorded on a Perkin-Elmer Lambda 20 UV−vis spectrometer and on a Shimadzu UV-160 spectrometer using dichloromethane as the solvent. IR spectra were recorded as KBr pellets on a Bruker Vector 22 FT IR spectrophotometer operating from 400 to 4000 cm^{-1}. Elemental analyses of the compounds were obtained from Thermoquest CE instruments CHNS-O, EA/110 model. FAB mass spectra were recorded on a JEOL SX 102/DA-6000 mass spectrometer/data system using argon/xenon (6kV, 10 mA) as the FAB gas. The accelerating voltage was 10 kV, and the spectra were recorded at room temperature. The ^1H, $^{31}P\{^1H\}$, and $^{13}C\{^1H\}$ NMR spectra were recorded in $CDCl_3$ solutions on a JEOL JNM LAMBDA 400 model spectrometer operating at 400.0, 161.7, and 100.4 MHz, respectively. Chemical shifts are reported in ppm with respect to internal tetramethylsilane (^1H and ^{13}C) and external 85% H_3PO_4 (^{31}P).

Magnetic Measurements. The magnetization of the powdered samples of **3**−**5** was assessed by SQUID (superconducting quantum interference device) measurements, using a Quantum Design MPMS-5 magnetometer, between 2 and 290 K in a constant field of 0.1 T. A cylindrical Teflon capsule was used as the sample holder which at 0.1 T yields a diamagnetic background of -4.70×10^{-5} emu + 5.07×10^{-5} emuK/T). Diamagnetic corrections were based on the experimentally derived susceptibility of the diamagnetic analogue $L_2(Zn(II))_3$ [$Zn_3C_{48}H_{48}N_{12}O_6P_2S_2$)] (**6**), $\chi_{dia} = -7.1 \times 10^{-4}$ emu/mol, by substituting the contribution of the three Zn(II) centers (-45×10^{-6} emu/mol) by the underlying diamgnetism and temperature-independent paramagnetism (TIP) of the paramagnetic M(II) centers.

X-ray Crystallography. The crystal data and the parameters for the compounds **2**−**4**, **5**, and **6** are given in Tables 1 and 2. Single crystals suitable for X-ray crystallographic analyses were obtained from slow evaporation of a solution of chloroform (**2**−**4**) or by vapor diffusing *n*-hexane into their chloroform solutions (**5** and **6**). The crystal data for compounds **3** and **6** were collected on a Bruker AXS Smart Apex diffractometer. The crystal data for compound **4** were collected on a Bruker P4 diffractometer, and the data for compounds **2** and **5** were collected on a Stoe IPDS machine. All structures were solved by direct methods using the programs SHELXS-97 and refined by full-matrix least-squares methods against F^2 with SHELXL-97.[10] Hydrogen atoms were fixed at calculated positions, and their positions were refined by a riding model. All non-hydrogen atoms were refined with anisotropic displacement parameters.

Synthesis. $(S)P[N(Me)NH_2]_3$ (1). Compound **1** was prepared by modifying a reported procedure.[11] $P(S)Cl_3$ (5.65 g, 33.4 mmol)

(4) (a) Trofimenko, S. *Chem. Rev.* **1993**, *93*, 943. (b) Parkin, G. *Adv. Inorg. Chem.* **1996**, *42*, 291. (c) Chen, P.; Root, D. E.; Campochiaro, C.; Fujisawa, K.; Solomon, E. I. *J. Am. Chem. Soc*. **2003**, *125*, 466. (d) Ruman, T.; Ciunik, Z.; Szklanny, E.; Woowiec, S. *Polyhedron* **2002**, *21*, 2743. (e) Puerta, D. T.; Cohen, S. M. *Inorg. Chem*. **2002**, *41*, 5075. (f) Long, D. P.; Chandrasekaran, A.; Day, R. O.; Binanconi, P. A.; Rheingold, A. L. *Inorg. Chem*. **2000**, *39*, 4476. (g) Fleming, J. S.; Psillakis, E.; Couchman, M. S.; Jeffery, J. C.; McCleverty, J. A.; Ward, M. D. *J. Chem. Soc., Dalton Trans*. **1998**, 537. (h) Jones, P. L.; Amoroso, A. J.; Jeffery, J. C.; McCleverty, J. A.; Psillakis, E.; Rees, L. H.; Ward, M. D. *Inorg. Chem.* **1997**, *36*, 10. (i) Rasika Dias, H. V.; Wang, Z.; Jin, W. *Inorg. Chem*. **1997**, *36*, 6205. (j) Rheingold, A. L.; Haggerty, B. S.; Yap, G. P. A.; Trofimenko, S. *Inorg. Chem.* **1997**, *36*, 5097.

(5) (a) Gade, L. H. *Eur. J. Inorg. Chem.* **2002**, 1257. (b) Gade, L. H. *J. Organomet. Chem.* **2002**, *661*, 85. (c) Veith, M. *Chem. Rev.* **1990**, *90*, 3. (d) Veith, M.; Weidner, S.; Kunze, K.; Käfer, D.; Hans, J.; Huch, V. *Coord. Chem. Rev.* **1994**, *137*, 297. (e) Brauer, D. J.; Bürger, H.; Liewald, G. R.; Wilke, J. *J. Organomet. Chem.* **1985**, *287*, 305.

(6) (a) Chandrasekhar, V.; Nagendran, S.; Kingsley, S.; Krishnan, V.; Boomishankar, R. *Proc. Indian Acad. Sci., Chem. Sci.* **2000**, *112*, 171. (b) Chandrasekhar, V.; Kingsley, S.; Vij, A.; Lam, K. C.; Rheingold, A. L. *Inorg. Chem*. **2000**, *39*, 3238. (c) Kingsley, S.; Vij, A.; Chandrasekhar, V. *Inorg. Chem.* **2001**, *40*, 6057. (d) Kingsley, S.; Chandrasekhar, V.; Incarvito, C. D.; Lam, M. K.; Rheingold, A. L. *Inorg. Chem.* **2001**, *40*, 5890. (e) Chandrasekhar, V.; Kingsley, S.; Rhatigen, B.; Lam, K. M.; Rheingold, A. L. *Inorg. Chem.* **2002**, *41*, 1030.

(7) (a) Caminade, A. M.; Majoral, J. P. *Chem. Rev.* **1994**, *94*, 1183. (b) Caminade, A. M.; Majoral, J. P. *Synth. Lett*. **1996**, 1019. (c) Mitjaville, J.; Caminade, A. M.; Daran, J. C.; Donnadieu, B.; Majoral, J. P. *J. Am. Chem. Soc*., **1995**, *117*, 1712. (d) Mitjaville, J.; Caminade, A. M.; Majoral, J. P. *Chem. Commun.* **1994**, 2161. (e) Gonce, F.; Caminade, A. M.; Boutonnet, F.; Majoral, J. P. *J. Org. Chem.* **1992**, *57*, 970. (f) Badri, M.; Majoral, J. P.; Caminade, A. N.; Delmas, M.; Gaset, A.; Gorgues, A.; Jaud, J. *J. Am. Chem. Soc*. **1990**, *112*, 5618.

(8) (a) Katti, K. V.; Reddy, V. S.; Singh, P. R. *Chem. Soc. Rev.* **1995**, *24*, 97. (b) Wang, M.; Volkert, E. W.; Singh, P. R.; Katti, K. K.; Lusiak, P.; Katti, K. V.; Barnes, C. L. *Inorg. Chem*. **1994**, *33*, 1184. (c) Singh, P. R.; Jimenez, H.; Katti, K. V.; Volkert, W. A.; Barnes, C. L. *Inorg. Chem*. **1994**, *33*, 736. (d) Reddy, V. S.; Katti, K. V.; Barnes, C. L. *Organometallics* **1994**, *13*, 2391. (e) Katti, K. V.; Ge, Y. W.; Singh, P. R.; Date, S. V.; Barnes, C. L. *Organometallics* **1994**, *13*, 541. (f) Katti, K. V.; Singh, P. R.; Barnes, C. L. *Inorg. Chem*. **1992**, *31*, 4588.

(9) *Vogel's Textbook of Practical Organic Chemistry*, 5th ed.; Longman: London, 1989.

(10) Sheldrick, G. M. *SHELXL-97, Program for crystal structure analysis*, release 97-2; University of Göttingen: Göttingen, Germany, 1998.

Table 1. Crystal and Structure Refinement Data for Compounds **2**−**4**

	LH_3 (**2**)	L_2Mn_3 (**3**)	L_2Co_3 (**4**)
empirical formula	$C_{25}H_{28}Cl_3N_6O_3PS$	$C_{51}H_{51}Cl_9Mn_3N_{12}O_6P_2S_2$	$C_{51}H_{51}Cl_9Co_3N_{12}O_6P_2S_2$
fw	629.92	1537.97	1549.94
T	213 (2) K	150 (2) K	293 (2) K
wavelength	0.71073 Å	0.71073 Å	0.71073 Å
cryst syst	triclinic	triclinic	monoclinic
space group	$P\bar{1}$	$P\bar{1}$	$P2_1/n$
unit cell dimensions	a = 10.184(2) Å	a = 11.048(6) Å	a = 11.259 (2) Å
	b = 10.895(2) Å	b = 11.100(6) Å	b = 27.027(2) Å
	c = 14.143(3) Å	c = 15.767(8) Å	c = 21.830(2) Å
	α = 96.83(3)°	α = 83.729(9)°	α = 90°
	β = 107.19(3)°	β = 72.136(9)°	β = 99.370(12)°
	γ = 100.30(3)°	γ = 62.092(7)°	γ = 90°
V, Z	1450.1(5) Å^3, 2	1624.9(14) Å^3, 1	6565.2(16) Å^3, 4
d (calcd)	1.443 Mg/m^3	1.572 Mg/m^3	1.568 Mg/m^3
abs coeff	0.482 mm^{-1}	1.114 mm^{-1}	1.283 mm^{-1}
F(000)	652	779	3140
cryst size	0.4 × 0.3 × 0.3 mm^3	0.4 × 0.3 × 0.16 mm^3	0.17 × 0.99 × 0.44 mm^3
θ range for data collection	1.93−22.86°	2.72−22.49°	2.04−27.50°
limiting indices	$-11 \le h \le 11$,	$-11 \le h \le 11$,	$-14 \le h \le 14$,
	$-11 \le k \le 11$,	$-11 \le k \le 11$,	$-34 \le k \le 33$,
	$-15 \le l \le 15$	$-16 \le l \le 15$	$-28 \le l \le 28$
reflns collected	5900	6359	14776
indep reflns	3536 (R_{int} = 0.0655)	4146 (R_{int} = 0.0362)	14184 (R_{int} = 0.0480)
completeness to θ	89.1%	97.8%	94.0%
refinement method	full-matrix least-squares on F^2	full-matrix least-squares on F^2	full-matrix least-squares on F^2
data/restraints/params	3536/0/358	4146/30/387	14184/0/827
GOF on F^2	1.000	1.015	1.017
final R indices [$I > 2\sigma(I)$]	R1 = 0.0503	R1 = 0.1138	R1 = 0.0591
	wR2 = 0.1374	wR2 = 0.3034	wR2 = 0.1385
R indices (all data)	R1 = 0.0724	R1 = 0.1347	R1 = 0.1119
	wR2 = 0.1515	wR2 = 0.3166	wR2 = 0.1660
largest diff peak and hole	0.346 and −0.498 e Å^{-3}	0.3360 and −1.078 e Å^{-3}	0.685 and −0.655 e Å^{-3}

Table 2. Crystal and Structure Refinement Data for Compounds **5** and **6**

	L_2Ni_3 (**5**)	L_2Zn_3 (**6**)
empirical formula	$C_{50}H_{50}Cl_6Ni_3N_{12}O_6P_2S_2$	$C_{52}H_{52}Cl_{12}Zn_3N_{12}O_6P_2S_2$
fw	1429.91	1688.63
T	213 (2) K	273 (2) K
wavelength	0.71073 Å	0.71073 Å
cryst syst	monoclinic	triclinic
space group	$C2/c$	$P\bar{1}$
unit cell dimensions	a = 18.866 (3) Å	a = 11.166 (6) Å
	b =11.7893(13) Å	b = 15.138 (8) Å
	c = 28.012 (4) Å	c = 21.243 (10) Å
	α = 90°	α = 72.971(8)°
	β = 107.175(18)°	β = 82.029(12)°
	γ = 90°	γ = 74.454(8)°
V, Z	5952.5(15) Å^3, 4	3301 (3) Å^3, 2
d (calcd)	1.596 Mg/m^3	1.699 Mg/m^3
abs coeff	1.391 mm^{-1}	1.737 mm^{-1}
F(000)	2920	1704
cryst size	0.5 × 0.4 × 0.4 mm^3	0.3 × 0.3 × 0.2 mm^3
θ range for data collection	2.06−24.24°	1.45−28.32°
limiting indices	$-21 \le h \le 21$	$-14 \le h \le 9$
	$-13 \le k \le 13$	$-19 \le k \le 16$
	$-32 \le l \le 32$	$-28 \le l \le 20$
reflns collected	18655	20802
indep reflns	4730 (R_{int} = 0.0549)	14443 (R_{int} = 0.0206)
completeness to θ	98.5%	87.8%
refinement method	full-matrix least-squares on F^2	full-matrix least-squares on F^2
data/restraints/params	4730/0/369	14443/186/808
GOF on F^2	0.963	1.037
final R indices [$I > 2\sigma(I)$]	R1 = 0.0322	R1 = 0.0700
	wR2 = 0.0768	wR2 = 0.2031
R indices (all data)	R1 = 0.0488	R1 = 0.0817
	wR2 = 0.0835	wR2 = 0.2140
largest diff peak and hole	0.396 and −0.487 e Å^{-3}	1.987 and −2.119 e Å^{-3}

dissolved in chloroform (75 mL) was added dropwise over a period of 1 h to a solution of *N*-methylhydrazine (9.31 g, 202.0 mmol) in chloroform (75 mL) maintained at 0 °C. The reaction mixture was allowed to come to room temperature over a period of 1 h and was further stirred for 10 h at this temperature. The precipitated *N*-methylhydrazine hydrochloride was filtered and the filtrate stripped off the solvent in vacuo to afford a white solid. This was

(11) Majoral, J. P.; Kraemer, R.; Navech, J.; Mathis, F. *Tetrahedron* **1976**, *32*, 2633.

Scheme 1

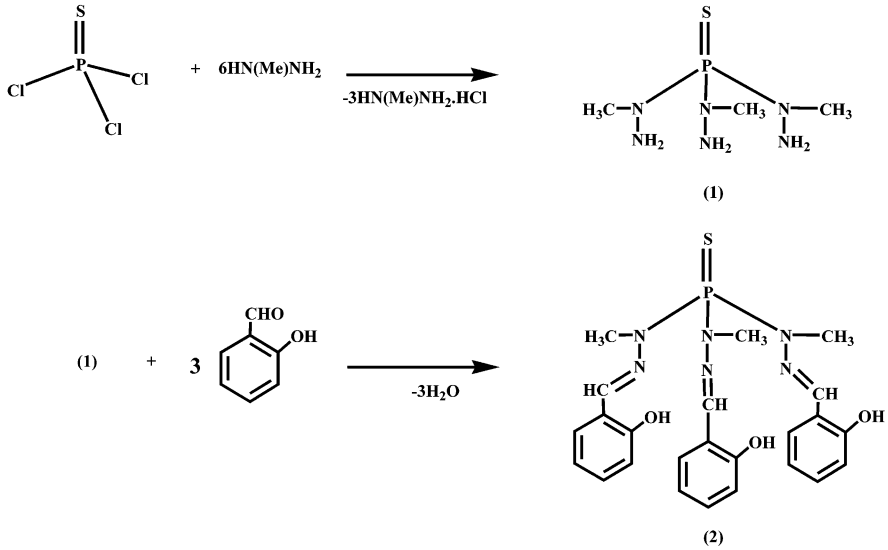

dissolved in hot benzene (75 mL) (*caution: benzene is a known carcinogen*) and cooled, and these steps were followed by the addition of *n*-hexane (125 mL). This mixture was kept at 5 °C to afford the title compound as a white crystalline compound. Yield: 5.41 g, 82.0%. Mp: 153−154 °C. ^{1}H NMR: 2.87 (d, 9H, −N(C*H*$_3$); $^3J(^1\text{H}-^{31}\text{P}) = 10.0$ Hz), 3.7 (broad, 6H, −N*H*$_2$). ^{31}P NMR: 84.5(s). FAB-MS: 198(M)$^+$.

(S)P[N(Me)N=CH−C$_6$H$_4$-*o*-OH]$_3$ (2). To a stirred solution of **1** (3.96 g, 20.0 mmol) in methanol (60 mL) was added dropwise a solution of salicylaldehyde (7.33 g, 60.0 mmol) also in methanol (60 mL) at room temperature. After the addition was over, the reaction mixture was heated under reflux for 10 h. A white solid that formed was filtered and recrystallized by dissolving it in boiling acetonitrile and allowing the resultant solution to cool to room temperature. This procedure afforded the title compound in a pure state. Yield: 8.98 g, 88.0%. Mp: 258 °C. UV−vis (CH_2Cl_2) λ_{max}/nm (ϵ/ L mol^{-1} cm^{-1}): 315 (28668), 287 (47238), 278 (45973). FT-IR $\nu_{C=N}$/cm^{-1}: 1606. ^{1}H NMR: 3.27 (d, 9H, −N(C*H*$_3$); $^3J(^1\text{H}-^{31}\text{P}) = 9.3$ Hz), 6.76−6.82 (m, 6H, aromatic), 7.10−7.18 (m, 6H, aromatic), 7.76 (s, 3H, imino), 10.53 (s, 3H, hydroxyl). ^{13}C NMR: 31.8 (N-*C*H$_3$), 116.8, 118.4, 119.3, 130.6, 143.4 (aromatic carbons), 157.3 (N=*C*H). ^{31}P NMR: 71.7(s). FAB-MS: 511 (M$^+$). Anal. Calcd for $C_{24}H_{27}N_6O_3PS$: C, 56.46; H, 5.33; N, 16.46. Found: C, 56.40; H, 5.21; N, 16.31.

Preparation of the Trinuclear Metal Complexes 3−6. The general procedure of preparation of the metal complexes is as follows. To a solution of ligand **2** (0.6 mmol) in chloroform (30 mL) was added dropwise a solution of the corresponding hydrated metal acetate (0.9 mmol) in methanol (30 mL) at room temperature, and the reaction mixture stirred for 6 h. The metal complex precipitated out of the reaction mixture and was filtered. This was dissolved in a minimum amount of dichloromethane (5 mL), and *n*-hexane was added to it until a slight turbidity appeared. This was kept at 5 °C to obtain a crystalline product. In the preparation of tri-manganese complex **3**, triethylamine(6 mmol) was added to ligand **2** prior to the addition of the metal acetate. The characterization data for these complexes are outlined in the following paragraphs.

{(S)P[N(Me)N=CH−C$_6$H$_4$-*o*-O]$_3$}$_2$Mn$_3$ (3). Yield: 0.26 g, 75.0%. Mp: 290 °C (d). UV−vis (CH_2Cl_2) λ_{max}/nm (ϵ/L mol^{-1} cm^{-1}): 362 (39383), 287 (63753). FT-IR $\nu_{C=N}$/cm^{-1}: 1595. FAB-MS: 1179(M$^+$). Anal. Calcd for $C_{48}H_{48}N_{12}O_6P_2S_2Mn_3$: C, 48.86; H, 4.10; N, 14.25. Found: C, 48.08; H, 4.13; N, 13.63.

{(S)P[N(Me)N=CH−C$_6$H$_4$-*o*-O]$_3$}$_2$Co$_3$ (4). Yield: 0.26 g, 74.3%. Mp: >295 °C. UV−vis (CH_2Cl_2) λ_{max}/nm (ϵ/ L mol^{-1} cm^{-1}): 373 (30943), 286 (53952). FT-IR $\nu_{C=N}$/cm^{-1}: 1599. ^{31}P NMR: 140.0 (s). FAB-MS: 1191 (M$^+$). Anal. Calcd for $C_{48}H_{48}N_{12}O_6P_2S_2Co_3$: C, 48.37; H, 4.06; N, 14.10. Found: C, 48.16; H, 3.99; N, 14.06.

{(S)P[N(Me)N=CH−C$_6$H$_4$-*o*-O]$_3$}$_2$Ni$_3$ (5). Yield: 0.27 g, 77.0%. Mp: >295 °C. UV−vis (CH_2Cl_2) λ_{max}/nm (ϵ/L mol^{-1} cm^{-1}): 383 (31624), 276 (54725). FT-IR $\nu_{C=N}$/cm^{-1}: 1600. ^{31}P NMR: −112.1(s). FAB-MS: 1190 (M$^+$). Anal. Calcd for $C_{48}H_{48}N_{12}O_6P_2S_2Ni_3$: C, 48.40; H, 4.06; N, 14.11. Found: C, 48.05; H, 4.00; N, 13.79;

{(S)P[N(Me)N=CH−C$_6$H$_4$-*o*-O]$_3$}$_2$Zn$_3$ (6). Yield: 0.27 g, 75.8%. Mp: >295 °C. UV−vis (CH_2Cl_2) λ_{max}/nm (ϵ/L mol^{-1} cm^{-1}): 316 (62434), 286 (103097), 278 (100280). FT-IR $\nu_{C=N}$/cm^{-1}: 1598. ^{1}H NMR: 3.38 (d, 9H, −N(C*H*$_3$); $^3J(^1\text{H}-^{31}\text{P}) = 11.0$ Hz), 6.23−6.43 (m, 6H, aromatic), 6.84−6.92 (m, 6H, aromatic), 8.20 (s, 3H, imino). ^{13}C NMR: 37.2 (N−*C*H$_3$), 114.9, 116.2, 122.9, 133.0, 133.5, 162.4 (aromatic carbons), 167.7 (N=*C*H). ^{31}P NMR: 67.0 (s). FAB-MS: 1211 (M$^+$). Anal. Calcd for $C_{48}H_{48}N_{12}O_6P_2S_2Zn_3$: C, 47.60; H, 3.99; N, 13.88. Found: C, 47.40; H, 3.74; N, 13.68.

Results and Discussion

Synthesis of Compounds 1−6. The reaction of P(S)Cl$_3$ with *N*-methylhydrazine affords the tris hydrazide P(S)-[N(Me)NH$_2$]$_3$ (**1**) as reported in the literature previously.[11] In this reaction, the *N*-methyl hydrazine itself is used as the hydrogen chloride scavenger. This reaction is regiospecific with the N−Me end of the hydrazine reagent reacting exclusively with the phosphorus compound. This leaves **1** with three reactive NH$_2$ groups for further derivatization. Condensation of **1** with 3 equiv of *o*-hydroxybenzaldehyde affords the tris hydrazone P(S)[N(Me)N=CH−C$_6$H$_4$-2-OH]$_3$ (LH$_3$) (**2**) (Scheme 1).

The conversion of **1** into **2** results in noticeable changes in some spectroscopic features. Thus, the ^{31}P{^{1}H} chemical shift observed in **1** at 84.5 ppm moves upfield to 71.7 ppm in **2**. Similarly, the N−CH$_3$ chemical shift in **1** that occurs at 2.87 ppm moves downfield to 3.27 ppm in **2**. A reduction of ^3J(P−H) is also noticed from 10.0 Hz (**1**) to 9.3 Hz (**2**). Finally, the IR spectrum of **2** is characterized by the strong

Scheme 2

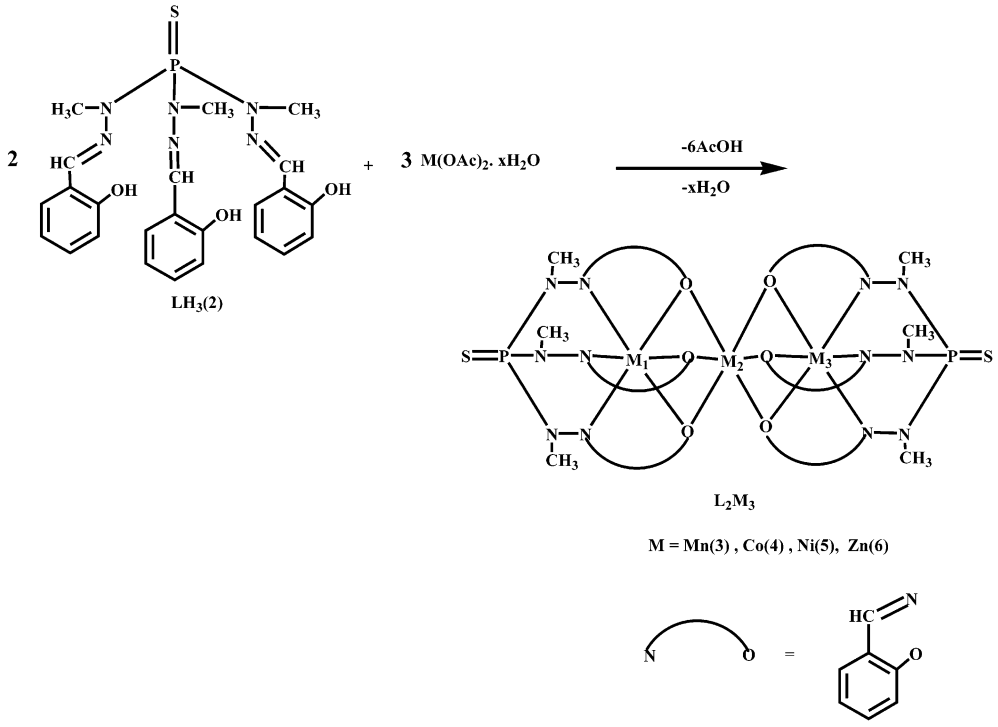

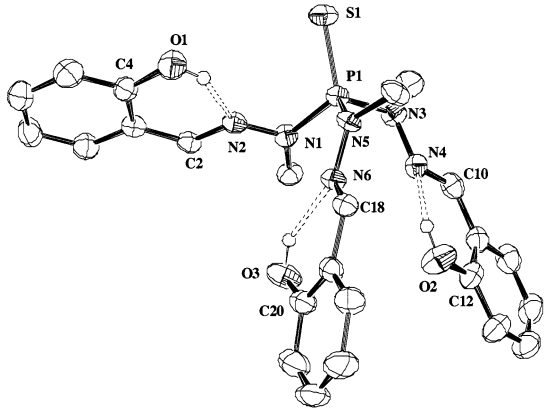

Figure 1. ORTEP diagram of LH_3 (**2**). Hydrogen atoms have been omitted for clarity.

absorption at 1606 cm^{-1} assigned to ν(C═N). These trends are similar to those observed in the conversion of cyclophosphazene hydrazides to ferrocene appended hydrazones.[12] The structure of **2** was further confirmed by an X-ray crystal structure determination (vide infra).

The multisite coordination ligand **2** has six potential sites for interacting with a transition metal ion: (1) three acidic phenolic sites and (2) three imino nitrogen centers. We have chosen metal acetates as convenient substrates for entry into the metal assemblies. Accordingly, the reaction of tris hydrazone **2** with $M(OAc)_2 \cdot xH_2O$ (M = Mn, Co, Ni, $x = 4$; and M = Zn, $x = 2$) proceeds very smoothly under mild reaction conditions to afford neutral trinuclear complexes **3**−**6** of the type L_2M_3 in very high yields (Scheme 2).

This reaction occurs by elimination of acetic acid and generation of the phenolate anions in situ. Interestingly, changing the stoichiometric ratio of the reactants does not lead to the isolation of any other product. All the trinuclear complexes show prominent parent ion peaks in their FAB mass spectra. The ν(C═N) in the complexes also does not alter significantly in comparison to the parent ligand **2**. The ^{31}P chemical shift of the diamagnetic L_2Zn_3 complex (+67.0 ppm) is upfield-shifted with respect to the ligand.

Table 3. A Comparison of Bond Length (Å) and Angles (deg) for Compounds **2**−**6**

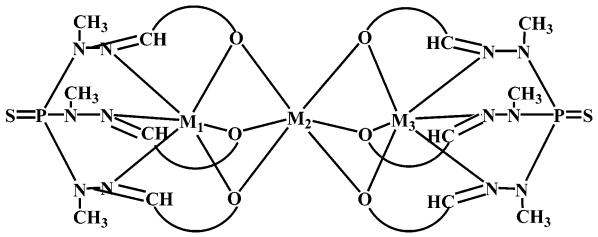

	LH_3 (**2**)	L_2Mn_3 (**3**)	L_2Co_3 (**4**)	L_2Ni_3 (**5**)	L_2Zn_3 (**6**)
P−S	1.9375(17)	1.938(4)	1.9276(17)	1.9286(11)	1.9375(2)
P−N	1.668(4)	1.686(11)	1.666(4)	1.676(3)	1.671(5)
N−N	1.388(5)	1.433(14)	1.440(5)	1.453(3)	1.435(6)
N═C	1.283(6)	1.294(16)	1.285(6)	1.286(4)	1.290(7)
$M_1(M_3)$−N		2.245(10)	2.105(4)	2.036(2)	2.151(4)
$M_1(M_3)$−O		2.133(8)	2.068(3)	2.038(19)	2.071(4)
M_2−O		2.197(8)	2.101(3)	2.072(19)	2.117(4)
$M_1(M_3)$−M_2		2.949(2)	2.8817(8)	2.7968(7)	2.8815(14)
			2.8755(8)		2.8653(15)
M_1−M_3		5.897	5.755	5.588	5.740
M_1−M_2−M_3		180.00(7)	176.67(3)	174.71(3)	174.30(3)

X-ray Crystal Structure of 2. The molecular structure of **2** is given in Figure 1. The metric parameters for this compound are summarized in Table 3. The multisite coordination arms of the tris hydrazone ligand are anchored to a tetrahedral phosphorus center.

(12) Chandrasekhar, V.; Senthil Andavan, G. T.; Nagendran, S.; Krishnan, V.; Azhakar, R.; Butcher, R. J. *Organometallics* **2003**, *22*, 976.

The three P−N bond distances P(1)−N(1), P(1)−N(3), and P(1)−N(5) [av 1.668(4) Å] are all slightly smaller than the single bond P−N distance of 1.70 Å.[13] Such a shortening of P−N distances has been observed in other instances. For example, in amino-cyclophosphazenes and cyclophosphazanes, the exocyclic P−N distances are slightly shorter than the ideal single bond distance. This has been attributed to negative hyperconjugation effects.[14] The observed N−N [av 1.388(5) Å] and C−N distances [av 1.283(6) Å] are normal for a N−N single bond and a C−N double bond, respectively.[15] The three phenolic hydrogens present are involved in intramolecular hydrogen bonding to the respective imino nitrogens of the hydrazone arms leading to the formation of a six-membered ring (N−C−C−C−O−H). The metric parameters involved in this interaction, viz., O···N (av.2.645 Å) and H···N distances (av 1.907 Å) and the O−H···N bond angles (av 145.9°), are in keeping with the hydrogen bonding trends observed in such types of interacting units.[16]

X-ray Crystal Structures of 3−6. The molecular structure of **4** is shown in Figure 2a. Compounds **3**, **5**, and **6** have similar structures. The ORTEP diagrams of these compounds are given in the Supporting Information. Table 3 gives the comparison of important bond parameters for all these compounds along with that of the ligand. Complexes **3**−**6** are trinuclear; each metal in the trinuclear assembly has an average oxidation state of +2. Two molecules of the tris hydrazone ligand are involved in coordination to the three metal ions in these complexes. Thus, each tris hydrazone molecule (LH_3) behaves as a tris chelating, trianionic hexadentate ligand $(L)^{3-}$, supplying three imino nitrogen atoms and three phenolate oxygen atoms for coordination to the metal ion. Of the three metal ions present in the molecular assembly, the two terminal metal ions (M_1 and M_3) have an N_3O_3 coordination environment while the central metal ion (M_2) has an O_6 coordination environment. The geometry around the metal centers (M_1 and M_3) is distorted octahedral with a N_3O_3 ligand set in a facial coordination mode [Figure 2b]. The geometry around M_2 is also distorted from an ideal octahedral arrangement.

Because of coordination to both terminal and central metal ions, each phenolate oxygen of the ligand acts as a bridging ligand in a μ_2 mode. As a result of this, two four-membered rings are formed connecting the terminal and central metal centers. Further, the coordination of the imino nitrogen and the phenolate oxygen leads to the formation of three [P−N−N-M−N−N] six-membered rings giving the overall appearance of a spherical cryptand [Figure 2c]. In all these trinuclear complexes, **3**−**6**, the three metal ions are arranged in a near linear manner (Figure 3). A paddle-wheel type of architecture is readily noticed by viewing the molecule along the intermetal axis [Figure 3b]. This type of arrangement has been observed in other linear trimetallic derivatives even though these latter complexes were assembled with entirely different types of ligands.[17] Thus, the paddle-wheel arrangement of the ligands may be viewed as a signature structural feature for linear trimetallic complexes.

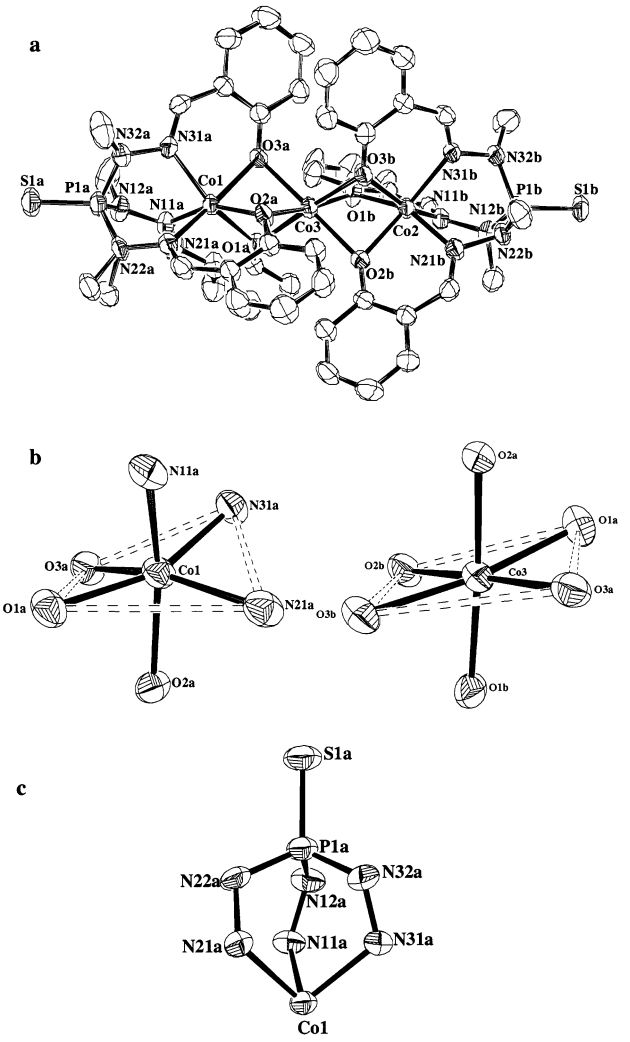

Figure 2. (a) ORTEP diagram of L_2Co_3 (**4**). Hydrogen atoms have been omitted for clarity. (b) The coordination environments around the terminal (Co1) and central (Co3) metal ions. (c) The six-membered [P−N−N−M−N−N] portion of the complex with a cryptand-like architecture.

Comparison of the Bond Parameters of 2−6 with Other Related Systems. Table 3 summarizes the metric parameters for ligand **2** and trimetallic complexes **3**−**6**. A comparison of the bond distances of **2** with **3**−**6** reveals that many bond distances (P−S, P−N, C−N) are largely unaffected by complexation. This is also corroborated by the invariance of the ν(C═N) upon complexation. The N−N bond distance of 1.388(5) Å increases slightly in complexes **3**−**6**. The M_1−N (M_3−N) distances although nearly constant show a

(13) Rademacher, P. *In Strukturen Organischer Molecüle*; VCH: Weinheim, 1987.
(14) Murugavel, R.; Krishnamurthy, S. S.; Chandrasekhar, J.; Nethaji, M. *Inorg. Chem.* **1993**, *32*, 5447.
(15) (a) Chandrasekhar, V.; Krishnan, V. *Adv. Inorg. Chem*. **2002**, *53*, 159. (b) Chandrasekhar, V.; Thomas, K. R. J. *Struct. Bonding* **1993**, *7*, 1.
(16) (a) Steiner, T. *Angew. Chem., Int. Ed.* **2002**, *41*, 48. (b) Desiraju, G. R.; Steiner, T. *The Weak Hydrogen Bond in Structural Chemistry and Biology*; Oxford Univeristy Press: Oxford, 1999. (c) Braga, D.; Polito, M.; Bracaccini, M.; D'Addario, D.; Tagliavini, E.; Sturba, L.; Grepioni, F. *Organometallics* **2003**, *22*, 2142.
(17) Clerac, R.; Cotton, F. A.; Daniels, L. M.; Dunbar, K. M.; Kirschbaum, K.; Murillo, C. A.; Pinkerton A. A.; Schultz, A. J.; Wang, X. *J. Am. Chem. Soc.* **2000**, *122*, 6226.

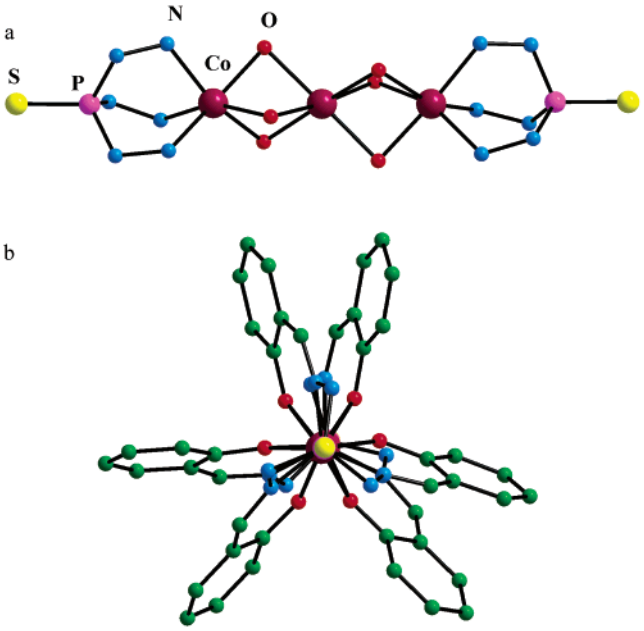

Figure 3. (a) Side view of the $(S)PN_3Co(\mu\text{-}O)_3Co(\mu\text{-}O)_3CoN_3P(S)$ core of L_2Co_3 (**4**). All the carbon atoms have been omitted for clarity. (b) Paddle-wheel type of arrangement of L_2Co_3 (**4**) as viewed through the intermetal axis. The $N-CH_3$ groups have been omitted for clarity.

slight variation depending on the type of metal ion. Thus, the largest distance is seen for the tri-manganese derivative (2.245(10) Å) while the shortest distance is seen for the tri-nickel complex (2.036(2) Å). In all the complexes, the $M_1(M_3)-O$ distance is shorter than the M_2-O distance. For each case, the longest distances are observed for the tri-manganese derivative. The linearity of the trimetallic array can be gauged by the $M_1-M_2-M_3$ angle. While the L_2Mn_3 complex shows a perfect linear arrangement (180°), in the corresponding L_2Co_3, L_2Ni_3, and L_2Zn_3 complexes this angle shrinks slightly.

A comparison of the structural features of the trimetallic derivatives with those known in the literature is instructive. A number of homo- and heterotrinuclear assemblies have been prepared by Cotton and co-workers[17,18] as well as by Wieghardt and co-workers[19,20] using dipyridylamine and substituted triazacyclononane ligands, respectively. There have also been reports on the preparation of trinuclear complexes by the use of 1,1,1-tris(*N*-salicylideneaminomethyl)ethane ligand.[21] Most of the trimetallic complexes prepared by Cotton and co-workers are neutral and are of the type $M_3(dpa)_4X_2$ (X = Cl, Br; M = Cu(II), Co(II), Cr(II), Ni(II)). In these complexes, the terminal and central metal ions have N_4X and N_4 coordination environments, respectively. Second, in these compounds, the presence of one M−M bond is also indicated. A comparison of the average terminal Co−N distance for $Co_3(dpa)_4X_2$ with those of the present study indicates the former has shorter Co−N distances (av 1.9847(3) Å).[18b] In contrast, the trinuclear complexes of Wieghardt are both neutral as well as cationic; both homo- as well as heterotrimetallic derivatives have been assembled. Further, in most of these complexes the terminal metal ions have a formal oxidation state of +3 while the central metal ions have +2 oxidation state. In general, in these derivatives the terminal metal ion has an N_3O_3 or N_3S_3 coordination environment while the central metal ion has an O_6 or S_6 coordination. The Ni(II)−N distance in the trimetallic complex $\{L'_2Ni(II),Ni(III),Ni(II)$ $\{L'H_3$ = 1,4,7-tris(4-*tert*-butyl-2-mercaptobenzyl)-1,4,7-triazacyclononane$\}$ is 2.096(9) Å, and it is comparable to the one observed in the present instance.[20] The metal−metal distances found for **3**−**6** (Table 2) suggest the absence of a M−M bond. Thus, in $Co_3(dpa)_4Cl_2$ where the presence of M−M bonds are indicated the average Co−Co distance is 2.3247(3) Å.[18b]

C−H···S Bond Assisted Supramolecular Architectures in 2−6. The molecular structures of **2**−**6** show several intermolecular interactions. Most of these are mediated through intermolecular C−H···S bonding. Although less investigated than the C−H···O interactions,[22] intermolecular C−H···S interactions are known to induce supramolecular formations.[23] Potrzebowski et al.[23a] have shown that C−H···S=P contacts are quite meaningful and have an influence on molecular packing. In a detailed study, these workers have observed that contacts (C···S) up to an upper limit of 4.08 Å could be considered. They have also indicated that in many such contacts the C−H···S angles are nonlinear. We have used these criteria to determine the presence and influence of C−H···S contacts in compounds **2**−**6**. Three representa-

(18) (a) Berry, J. F.; Cotton, F. A.; Daniels, L. M.; Murillo, C. A.; Wang, X. *Inorg. Chem.* **2003**, *42*, 2418. (b) Clerac, R.; Cotton, F. A.; Daniels, L. M.; Dunbar, K. R.; Murillo, C. A.; Wang, X. *Inorg. Chem.* **2001**, *40*, 1256. (c) Clerac, R.; Cotton, F. A.; Daniels, L. M.; Dunbar, K. R.; Murillo, C. A.; Wang, X. *J. Chem. Soc., Dalton Trans.* **2001**, 386. (d) Clerac, R.; Cotton, F. A.; Dunbar, K. M.; Lu, T.; Murillo, C. A.; Wang, X. *J. Am. Chem. Soc.* **2000**, *122*, 2272. (e) Clerac, R.; Cotton, F. A.; Dunbar, K. R.; Murillo, C. A.; Pascual, I.; Wang, X. *Inorg. Chem.* **1999**, *38*, 2655. (f) Cotton, F. A.; Daniels, L. M.; Murillo, C. A.; Pascual, I. *J. Am Chem. Soc.* **1997**, *119*, 10223. (g) Berry, J. F.; Cotton, F. A.; Lei, P.; Murillo, C. A. *Inorg. Chem.* **2003**, *42*, 377.

(19) (a) Auerbach, U.; Stockheim, C.; Weyhermüller, T.; Wieghardt, K.; Nuber, B. *Angew. Chem., Int. Ed. Engl.* **1993**, *32*, 714. (b) Krebs, C.; Glaser, T.; Bill, E.; Weyhermüller, T.; Meyer-Klaucke, W.; Wieghardt, K. *Angew. Chem., Int. Ed.* **1999**, *38*, 359. (c) Burdinski, D.; Bothe, E.; Wieghardt, K. *Inorg. Chem.* **2000**, *39*, 105. (d) Glaser, T.; Beissel, T.; Weyhermüller, T.; Schünemann, V.; Meyer-Klaucke, W.; Trautwein, A. X.; Wieghardt, K. *J. Am. Chem. Soc.* **1999**, *121*, 2193. (e) Albela, B.; Bill, E.; Brosch, O.; Weyhermüller, T.; Wieghardt, K. *Eur. J. Inorg. Chem.* **2000**, 139. (f) Glaser, T.; Kesting, F.; Beissel, E.; Bill, E.; Weyhermüller, T.; Meyer-Klaucke, W.; Wieghardt, K. *Inorg. Chem.* **1999**, *38*, 722. (g) Glaser, T.; Bill, E.; Weyhermüller, T.; Meyer-Klaucke, W.; Wieghardt, K. *Inorg. Chem.* **1999**, *38*, 2632. (h) Albela, B.; Bothe, E.; Brosch, O.; Mochizuki, K.; Weyhermüller, T.; Wieghardt, K. *Inorg. Chem.* **1999**, *38*, 5131.

(20) Beissel, T.; Birkelbach, F.; Bill, E.; Glaser, T.; Kesting, F.; Krebs, C.; Weyhermüller, T.; Wieghardt, K.; Butzlaff, C.; Trautwein, A. X. *J. Am. Chem. Soc.* **1996**, *118*, 12376.

(21) Ohta, H.; Harada, K.; Irie, K.; Kashino, S.; Kambe, T.; Sakane, G.; Shibahara, T.; Takamizawa, S.; Mori, W.; Nonoyama, M.; Hirotsu, M.; Kojima, M. *Chem. Lett.* **2001**, 842.

(22) (a) Thallapally, P. K.; Katz, A. K.; Carrell, H. L.; Desiraju, G. R. *CrystEngComm.* **2003**, *5* (18), 87. (b) Vishweshwar, P.; Thaimattam, R.; Jaskolski, M.; Desiraju, G. R. *Chem. Commun.* **2002**, 1830. (c) Chandrasekhar, V.; Nagendran, S.; Bansal, S.; Cordes, A. W.; Vij, A. *Organometallics* **2002**, *21*, 3297. (d) Desiraju, G. R. *Acc. Chem. Res.* **2002**, *35*, 565. (e) Desiraju, G. R. *Acc. Chem. Res.* **1996**, *29*, 441.

(23) (a) Potrzebowski, M. J.; Michalska, M.; Koziol, A. E.; Kazmierski, S.; Lis, T.; Pluskowski, J.; Ciesielski, W. *J. Org. Chem.* **1998**, *63*, 4209. (b) Chandrasekhar, V.; Baskar, V.; Kingsley, S.; Nagendran, S.; Butcher, R. J. *CrystEngComm* **2001**, *17*, 1. (c) Muralidharan, K.; Venugopalan, P.; Elias, A. J. *Inorg. Chem.* **2003**, *42*, 3176.

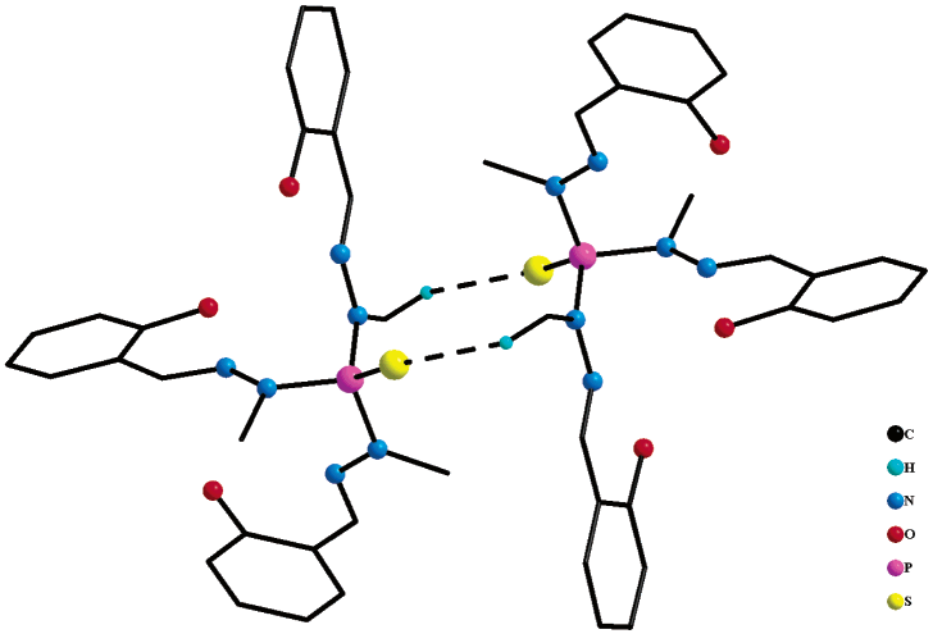

Figure 4. Intermolecular C—H···S═P contacts in **2**. All the hydrogen atoms which are not involved in the hydrogen bonding have been omitted for clarity. The metric parameters for the C(1)—H(1c)···S(1) contacts are C(1)—H(1c) 0.980(14) Å, H(1c)···S(1) 2.912(44) Å, C(1)···S(1) 3.649(59) Å and C(1)—H(1c)···S(1) 132.8(3)°. The symmetry is $1 - x, -y, 2 - z$.

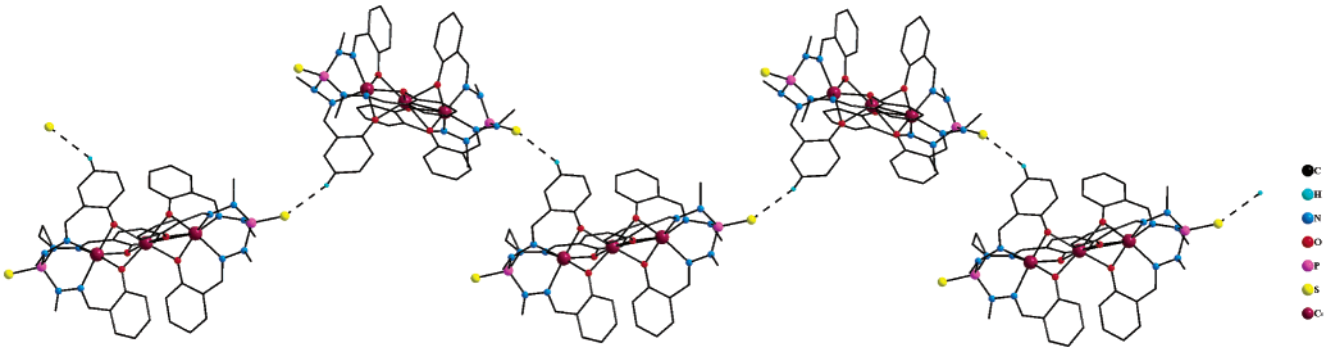

Figure 5. Intermolecular C—H···S═P assisted polymeric array in **4** leading to the formation of a zigzag polymeric chain. All the hydrogen atoms which are not involved in the hydrogen bonding have been omitted for clarity. The metric parameters for the C(15A)—H(15A)···S(1B) contact are C(15A)—H(15A) 0.929(8) Å, H(15A)···S(1B) 2.975(7) Å, C(15A)···S(1B) 3.739(13) Å, and C(15A)—H(15A)···S(1B) 140.53(37)°. The symmetry is $2.5 - x, -0.5 + y, 1.5 - z$.

tive examples (**2**, **4**, and **5**) are discussed here. The rest of the data are given in the Supporting Information.

Compound **2** forms a dimer as a result of a pairwise P═S···H—C bond between the P═S of one molecule with the hydrogen of the N—CH_3 moiety of another (Figure 4). The C—H···S angle is 132.8°, while the H···S and C···S distances are 2.912 and 3.649 Å, respectively. Compound **2** also shows other intermolecular interactions including $\pi-\pi$, C—H···π, C—H···O, and C—H···Cl contacts (Supporting Information).

All the trinuclear complexes have the P═S units at two opposite ends of the molecule, and these are prominently involved in C—H···S contacts. In the case of L_2Co_3 complex **4**, one C—H···S contact is present at each end. Thus, at one end of the molecule a proton donor interaction occurs through the aromatic proton (*para* to the phenolate oxygen). At the other end, a proton acceptor interaction occurs at the P═S location. The result is the formation of a zigzag polymeric chain (Figure 5).

In contrast to **4**, the L_2Ni_3 complex has a pair of C—H···S contacts at each end of the molecule. The interacting protons in this instance are imino (CH═N) protons This leads to the formation of a double-bridged zigzag polymeric chain (Figure 6). The supramolecular arrangement in tri-manganese complex **3** is similar to that found in **4** except that the interacting protons are derived from the N—CH_3 group (Supporting Information).

The L_2Zn_3 (**6**) complex has analogous intermolecular contacts to those of the L_2Co_3 derivative with the difference being that imino protons are involved in proton donor interactions. However, the presence of the solvent chloroform in the crystal lattice of L_2Zn_3 takes the one-dimensional polymeric chain into the second dimension by means of C—H···Cl contacts.[24] Thus, a chlorine atom of the solvent is involved in a bifurcated hydrogen bond with the N—CH_3

(24) (a) Thallapally, P. K.; Nangia, A. *CrystEngComm.* **2001**, *27*, 1. (b) Chandrasekhar, V.; Athimoolam, A.; Reddy, N. D.; Nagendran, S.; Steiner, A.; Zacchini, S.; Butcher, R. *Inorg. Chem.* **2003**, *42*, 51.

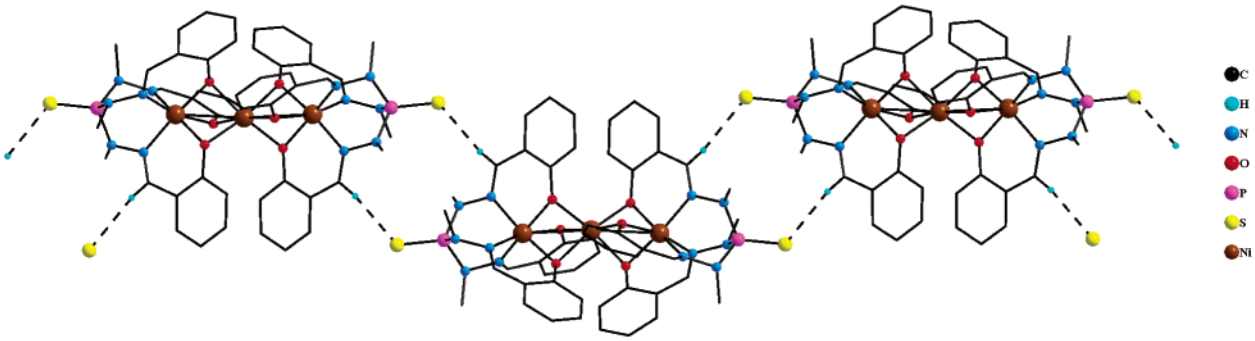

Figure 6. Intermolecular C—H···S═P interactions in **5**. All the hydrogen atoms which are not involved in the hydrogen bonding have been omitted for clarity. The metric parameters for the C(10)—H(10)···S(1) contact are C(10)—H(10) 0.940(6) Å, H(10)···S(1) 2.914(8) Å, C(10)···S(1) 3.844(13) Å and C(10)—H(10)···S(1) 170.51(19)°. The symmetry is 1.5 − *x*, 0.5 − *y*, 1 − *z*.

Scheme 3

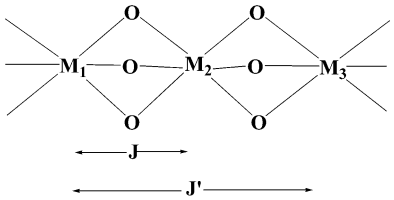

proton of a neighboring molecule and an aromatic C—H of another neighbor. The cumulative effect of the C—H···S and the C—H···Cl interactions is the formation of a two-dimensional supramolecular grid (Supporting Information).

Magnetic Properties. Magnetic measurements on complexes **3**−**5** feature both antiferro- and ferromagnetic exchange depending on the actual spin center M. Thus, in the L_2Mn_3 (**3**) and L_2Co_3 (**4**) complexes antiferromagnetic coupling is observed while for the L_2Ni_3 complex (**5**) a ferromagnetic coupling is observed between the adjacent nickel centers and an antiferromagnetic coupling is observed between the two terminal nickel centers.

The measured susceptibility functions were modeled using a simple Heisenberg isotropic exchange model that includes symmetric nearest-neighbor Heisenberg exchange between the central metal center M_2 and the two outer metal centers M_1 and M_3, $J = J_{12} = J_{23}$, and the next-nearest exchange between the outer metal positions, $J' = J_{13}$ (Scheme 3). To derive the spin energy levels and the magnetic thermodynamic properties for all systems discussed in the following paragraphs, numerical full-matrix-diagonalization has been carried out using a modified version of the MAGPACK program package.[25] The latter was adapted to allow for Levenberg−Marquardt least-squares fitting to obtain the relevant parameters. Despite slight differences of the coordination geometries (see Figure 2b), uniform *g* factors and zero-field splitting parameters were assumed for all three metal centers.

The observed magnetic data for the $(s = {}^5/_2)_3$ $L_2(Mn(II))_3$ derivative is well reproduced with the Heisenberg−Dirac−van Vleck-type Hamiltonian $\hat{H}_{HDvV} = -2J(\hat{S}_1\hat{S}_2 + \hat{S}_2\hat{S}_3) - 2J'\hat{S}_1\hat{S}_3$ for both an antiferromagnetic nearest- and next-nearest-neighbor exchange, $J = -4.0$ K and $J' = -0.15$ K, and a *g* factor of 1.99 (Figure 7).

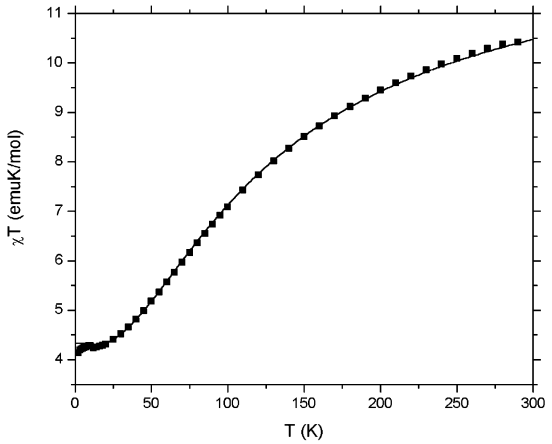

Figure 7. Temperature dependence of χT for the $L_2Mn_3[LMn^{II}Mn^{II}Mn^{II}L]$ complex, **3**. (Squares: experimental values. Gray curves: calculated values.)

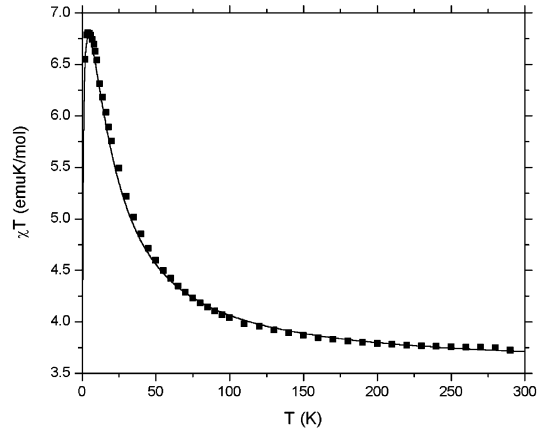

Figure 8. Temperature dependence of χT for the $L_2Ni_3[LNi^{II}Ni^{II}Ni^{II}L]$ complex, **5**. (Squares: experimental values. Gray curves: calculated values.)

This behavior is analogous to the one observed for similar linear Mn(II) trimers.[19c,26] In contrast, the $(s = 1)_3$ $L_2(Ni(II))_3$ derivative displays ferromagnetic nearest-neighbor and antiferromagnetic next-nearest-neighbor exchange interactions,

(25) Borrás-Almenar, J. J.; Clemente-Juan, J. M.; Coronado, E.; Tsukerblat, B. S. *J. Comput. Chem.* **2001**, *22*, 985

(26) (a) Menage, S.; Vitols, S. E.; Bergerat, P.; Codjovi, E.; Kahn, O.; Girerd, J. J.; Guillot, M.; Solans, X.; Calvet, T. *Inorg. Chem.* **1991**, *30*, 2666. (b) Rardin, R. L.; Poganiuch, P.; Bino, A.; Goldberg, D. P.; Tolman, W. B.; Liu, S.; Lippard, S. J. *J. Am. Chem. Soc.* **1992**, *114*, 5240. (c) Baldwin, M. J.; Kampf, J. W.; Kirk, M. L.; Pecoraro, V. L. *Inorg. Chem.* **1995**, *34*, 5252. (d) Tangoulis, V.; Malamatari, D. A.; Soulti, K.; Stergiou, V.; Raptopoulou, C. P.; Terzis, A.; Kabanos, T. A.; Kessissoglou, D. P. *Inorg. Chem.* **1996**, *35*, 4974. (e) Zhong, Z. J.; You, X. *Polyhedron* **1994**, *13*, 2157.

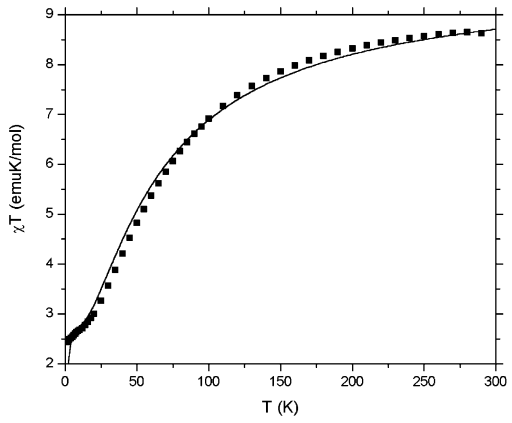

Figure 9. Temperature dependence of χT for the $L_2Co_3[LCo^{II}Co^{II}Co^{II}L]$ complex, **4**. (Squares: experimental values. Gray curves: calculated values.)

which results in a maximum of the χT versus T graph at approximately 4 K (Figure 8). Here, the Hamiltonian has to be extended to account for a single-ion anisotropy term (reflecting the zero-field splitting of the $^3A_2$ ground state), $\hat{H} = \hat{H}_{HDvV} + \hat{S}_1 D \hat{S}_1 + \hat{S}_2 D \hat{S}_2 + \hat{S}_3 D \hat{S}_3$, for which a best fit of $|D| = 1.1$ K is found. The exchange constants are established for an isotropic g factor of 2.17 to be $J = 4.43$ K and $J' = -0.28$ K. The magnetic behavior of the L_2Ni_3 derivative is similar to that observed in $[Ni(acac)_2]_3$[27] as well as in $Ni_3L''_2$ [L″ = 1,4,7-tris(3,5-dimethyl-2-oxybenzyl)-1,4,7-triazacyclononane].[20]

If the same simple Heisenberg model is also applied to the $L_2(Co(II))_3$ derivative, that displays only antiferromagnetic exchange and for which large anisotropy effects are expected due to first-order spin−orbit splitting of the cobalt $^4T_1$ ground state, one obtains satisfying yet less accurate fit for $J = -4.5$, $J' = -1.4$, $g = 2.64$, and $|D| = 5.0$ K (Figure 9).

(27) Ginsberg, A. P.; Martin, R. L.; Sherwood, R. C. *Inorg. Chem.* **1968**, *5*, 932.

In all of the three systems discussed here, deviations of the calculated susceptibilities from the measured values at low temperatures might be attributed to intermolecular interactions due to the aforementioned hydrogen bonds.

Conclusion

Phosphorus based trihydrazone ligand LH_3 is a robust multisite coordination ligand unlike the previously known phosphorus pyrazolide ligands. By using LH_3, it has been possible to assemble four trinuclear linear metal assemblies. While it appears that the ligand **2** should be able to generate trinuclear metal assemblies with many other metal ions (in an oxidation state of +2), this needs to be tested. The magnetic measurements carried out on **3**−**5** indicate that the phosphorus based trishydrazone ligand **2** provides a framework for diverse magnetic molecules. Depending on the embedded transition metal ion, the ligand can efficiently facilitate both antiferro- and ferromagnetic superexchange between neighboring metal centers. Due to antiferromagnetic next-nearest-neighbor interactions, all of the magnetically characterized complexes are assumed to display an $S = 0$ ground state. Forthcoming heterotrinuclear systems featuring mixtures of different spin centers might therefore result in high-spin ground states.

Acknowledgment. We thank Council of Scientific and Industrial Research, New Delhi, for supporting this research as well as providing senior research fellowships (G.T.S, V.K.).

Supporting Information Available: Tables (S1−S2) and additional figures (S1−S6). Crystallographic data in CIF format. This material is available free of charge via the Internet at http://pubs.acs.org.

IC034434H